

To appear in *ApJ Lett.*

Observational evidence for a correlation between peak-luminosities and beaming in GRBs

Maurice H.P.M. van Putten¹ and Tania Regimbau¹

LIGO Laboratory, NW 17-161, 175 Albany Street, Cambridge, MA 02139

ABSTRACT

We calculate the unseen-but-true GRB-event rate from a current flux-limited sample of 33 GRBs with individually measured redshifts. We consider a GRB-event rate which is proportional to the star-formation rate, in view of the GRB-SNe association in SN1998bw and GRB030329. By fitting a log-normal distribution of GRB peak-luminosities, we find a ratio $1/f_r \simeq 450$ for the true-to-observed GRB-event rates. This provides an independent derivation of the GRB-beaming factor $1/f_b \simeq 500$ obtained by Frail et al. (2001) from sources with standard GRB-energies. We discuss applications to GRB980425.

Subject headings: gamma-rays: bursts, beaming

1. Introduction

New clues are emerging that long GRB are associated with supernovae (Galama et al. 1998; Bloom et al. 1999; Kulkarni et al. 2000; Reichart 2001). This is illustrated most recently by optical emissions lines in the late-time light-curve of the HETE-II burst GRB 030329 (Stanek et al. 2003), which are remarkably similar to those observed in GRB980425/SN1998bw (Galama et al. 1998). A GRB-supernova association provides important support for the collapsar model of GRBs, representing a violent death of evolved massive stars (Woosley 1993; Paccynski 1998). The short lifespan of tens of Myrs of massive stars implies that GRBs take place in star-forming regions (Paccynski 1998; Fruchter et al. 1999), and hence more broadly points towards an association to molecular clouds. The event rate of GRBs per unit cosmological volume is hereby expected to be correlated to the cosmic star-formation rate (e.g., Blain & Natarajan (2000); Berger et al. (2003); Choudhury & Srianand (2002)). Because observations by past and current experiments (see Table I) are flux-limited, the observed GRB-event rate is strongly biased towards events at lower redshifts.

In this letter, we calculate the ratio $1/f_r$ of unseen-to-observed GRBs. Our analysis is based on the bias in the observed GRB-event rate towards low redshift events in a flux-limited sample of 33 GRBs with individually measured redshifts. We propose to use a linear relationship for the correlation between the true-but-unseen GRB event rate and the cosmic SFR, to derive from this bias a best-fit log-normal GRB peak-luminosity function. While it is an open question to what the degree cosmological evolution of metallicity affects the SFR independently of the GRB event rate (see, e.g., Heger et al. (2002)), linear relationship between the two will serve as a leading-order approximation.

In §2, we discuss the cosmological model. §3 tabulates the current sample of 33 GRBs with individually measured redshifts. In §4, we present the best fit of the data for a log-normal distribution function, estimate the fraction of unseen-to-observed GRBs, and compare our results with the beaming factor $1/f_b = 500$ of Frail et al. (2001), based on a sample of GRBs with achromatic breaks in their light-curves. We summarize our results and draw our main conclusions in §5.

2. The cosmological model

We model the intrinsic GRB-event rate in a flat Λ -dominated cold dark matter cosmology with closure energy densities $\Omega_\Lambda = 0.70$ and $\Omega_m = 0.30$. These values are suggested by BOOMERANG and MAXIMA (de Bernardis et al. 2000; Hanany et al. 2000) on the power spectra of the CMB and distant Type Ia SNe (Perlmutter et al. 1999; Schmidt et al. 1998). The Hubble parameter H_0 is taken to be $73 \text{ km s}^{-1} \text{Mpc}^{-1}$ (Freedman et al., 2001).

Porciani & Madau (2001) provide three models of the cosmic SFR up to redshifts $z \sim 5$, reflecting some uncertainties in SFR estimates. No significant changes have been noticed in application of these three models, and we present only results derived from the second model, SFR2. We have

$$R_c(z) = R_{SF2}(z) \frac{E(\Omega_i, z)}{(1+z)^{3/2}} \text{ M}_\odot \text{ yr}^{-1} \text{ Mpc}^{-3} \quad (1)$$

by transformation of the R_{SF2} in a matter-dominated universe ($\Omega_m = 1$),

$$R_{SF2}(z) = \frac{0.15 e^{3.4z}}{(22 + e^{3.4z})} \text{ M}_\odot \text{ yr}^{-1} \text{ Mpc}^{-3}, \quad (2)$$

where $E(\Omega_i, z) = [(1+z)^2(1+z\Omega_m) - z(2+z)\Omega_v]^{1/2}$.

For a GRB-event rate locked to the SFR, the true event rate between z and $z + dz$, as

observed in the observer’s frame of reference, satisfies

$$dR_{GRB}(z) = \lambda_{GRB} \frac{R_c(z)}{1+z} \frac{dV}{dz} dz \quad (3)$$

where λ_{GRB} is the formation mass fraction of the source progenitors. Here, the division by $1+z$ accounts for time-dilatation by cosmic expansion. The element of comoving volume is

$$dV = \frac{4\pi r^2 c}{H_0 E(\Omega_i, z)} dz, \quad r(z) = \int_0^z \frac{c}{H_0 E(\Omega_i, z')} dz' \quad (4)$$

The GRB redshift probability density can be written as (Coward et al. 2002) $p(z) = dR_{GRB}/dz \left(\int_0^5 dR_{GRB}/dz dz \right)^{-1}$. Assuming that the mass fraction of GRBs progenitors is redshift independent, the scaling factor λ_{GRB} is the only free parameter of our model. For the flux-limited experiments listed in Table I we define a probability-density function of detection as a function of redshift as $p_{detect}(z) = dR_{detect}/dz \left(\int_0^5 dR_{detect}/dz dz \right)^{-1}$, where the dependence on the luminosity has been integrated out in the detected event rate (Bromm & Loeb 2002)

$$dR_{detect} = dR_{GRB}(z) \int_{L_{lim}(z)} p(L) dL \quad (5)$$

Here, $p(L)$ refers to the intrinsic GRBs luminosity function in the BATSE energy range 50 – 300 keV.

The luminosity threshold as a function of redshift is given by $L_{lim}(z) = 4\pi d_L^2(z) S_{lim}$, where d_L is the luminosity distance to a source at redshift z and where S_{lim} denotes the sensitivity threshold of the instrument. Following (Bromm & Loeb 2002), we take a flux-density threshold of BASTE of 0.2 photon cm⁻² s⁻¹.

3. A redshift sample of 33 GRBs

As of the time of this writing, we have 33 GRBs with individually measured redshifts (Table I). They collectively represent a variety of past and current experiments. Due to a flux threshold in each of the instruments used, the observed GRB redshift distribution is strongly biased towards low redshifts. This introduces a quantitative selection effect, relative to the redshift distribution predicted by the SFR model (Fig. 1) – the true distribution of GRB-redshifts representing what would be observed in the ideal case of a zero-flux threshold in the instruments. In view of the various instruments involved, the dependency of the observed GRB redshift-distribution function on the flux-limit is simulated in Fig. 2.

4. A fit to a log-normal distribution function

We shall assume that the GRB-luminosity function is redshift independent, i.e., without cosmological evolution of the nature of its progenitors. We take a log-normal probability density for the luminosity shape-function, with mean μ and width σ given by

$$p(L) = \frac{1}{(2\pi)^{1/2}\sigma L} \exp\left(\frac{-(\ln L - \mu)^2}{2\sigma^2}\right), \quad (6)$$

where L is normalized with respect to $1\text{cm}^{-2}\text{s}^{-1}$. The optimized parameters of our model are

$$(\mu, \sigma) = (124, 3) \pm (2, -0.4). \quad (7)$$

This notation means that the estimated parameters can be either (122,3.4), (123,3.2), (125,2.8), or (126,2.6), but not (122,2.6) for instance. Our results are compatible to the expectations of Sethi et Bhargavi (2001) who derive a log-normal luminosity function with $\mu = 129$ and $\sigma = 2$ from a different flux-limited sample. They mentioned that because of selection effects, the inferred average luminosity over-estimates the true mean luminosity by a factor of 2 or 3, and the variance is within 40-50% of the true variance. The observed and predicted redshift distribution, based on the SFR, are shown in Fig. 1 in case of optimal parameters (7). The results indicate a good fit to the data, suggesting that selection effects are adequately modeled. The fraction of *detectable* GRBs as a function of redshift

$$F(z) = \frac{dR_{\text{detect}}}{dR_{\text{GRB}}(z)} = \int_{L_{\text{lim}}(z)} p(L) dL. \quad (8)$$

shows a the steep decrease as the luminosity threshold increases, making high-redshift GRBs less likely to be detected.

A satisfactory test for our model is provided by comparing the predicted flux distribution of GRBs above the sensitivity threshold with the peak flux distribution of a sample of 67 GRBs observed with IPN (Fig. 3). The fluxes derived from our luminosity function in 50-300 keV have been extrapolated to the IPN range of 25-100 keV, assuming an E^{-2} energy spectrum and using the formula given in Appendix B of Sethi et Bhargavi (2001). The conversion factor from $\text{erg cm}^{-2} \text{s}^{-1}$ to $\text{photon cm}^{-2} \text{s}^{-1}$ has been taken to be 0.87×10^{-7} , and the sensitivity threshold equal to 5 $\text{photon cm}^{-2} \text{s}^{-1}$ (Hurley, private communication).

A quantitative result provided by our model is the ratio $1/f_r$ of the true GRB-event rate (what would be seen in case of a zero-flux limit in the detector) and the observed GRB-event rate. For the optimal parameters (7), we have

$$1/f_r = 450. \quad (9)$$

The factor $1/f_r$ is between 200-1200 in the error box of (7).

5. A correlation between $1/f_r$ and $1/f_b$

Our estimate of the true-to-observed GRB-event rate $1/f_r$ is strikingly similar to the GRB-beaming factor $1/f_b$ of about 500 derived by Frail et al. (2001). Our analysis is independent of the mechanism providing a broad distribution in GRB luminosities. Without further input, our results may reflect (a) isotropic sources with greatly varying energy output, (b) beamed sources with standard energy output and varying opening angles, or (c) anisotropic but geometrically standard sources (Rossi et al. 2002; Zhang & Meszaros 2002).

We find that the GRB peak-luminosities and beaming are correlated. To see this, we simply note that the case of no correlation between peak-luminosities and beaming give rise to an unseen-but-true GRB event rate which is $1/f_r \times 1/f_b \simeq 2.5 \times 10^5$ times the observed rate. The true GRB-event rate hereby approaches that of Type II supernovae – we discard this possibility. A correlation between peak-luminosities and beaming is naturally expected sources (b) and (c) with standard energy output – the picture that bears out of Frail et al. (2001). This introduces a correlation $L \propto 1/f_b$ between peak-luminosity and beaming factor in (b) and, for a flux-limited sample, also in (c). For a flux-limited sample, both (b) and (c) give rise to an anticorrelation between inferred beaming and distance such that to leading-order $\theta_j z \sim \text{const.}$ Fig. 4 shows that this anticorrelation holds in the sample of Frail et al. (2001). For a related discussion on estimating the GRB beaming factor from flux limited surveys, see Levinson et al. (2002).

6. Conclusions

A table of 33 GRBs with individually determined redshifts allows an estimate of the GRB-luminosity function, based on constant of proportionality between the GRB event rate and the cosmic star-formation rate. We have tested our fit by reproducing the distribution of peak luminosities in the IPN sample of 67 GRBs.

A flux-limited sample introduces a ratio $1/f_r$ of unseen GRBs, whose emissions fall below the detector threshold, to observed GRBs. A best fit analysis of the luminosity function gives $1/f_r \simeq 450$. This number is both large and close to the GRB beaming factor of 500. The possibility that $1/f_r$ and $1/f_b$ are uncorrelated gives rise to prohibitively large true GRB event rates, and is discarded. The results support a relation $L \propto 1/f_b$ between the peak-luminosity and the beaming factor in the context of conical or anisotropic GRB-emissions with standard GRB-energies. This points towards an anticorrelation between distance and half-opening angle, which is approximately supported by the sample of Frail et al. (2001).

The results presented here and those of Frail et al. (2001) indicate a true GRB event

rate of 1 per year within $D = 100\text{Mpc}$. GRB980425/SN1998bw ($z = 0.0085$) is consistent with this true event rate. For anisotropic but geometrically standard sources, GRB980425 is hereby *not* anomalous, but consistent with the trend shown in Fig. 4.

The authors greatfully acknowledge input from Kevin Hurley. MVP thanks R. Mochkovitch for discussions on GRB980425. This research is supported by the LIGO Observatories, constructed by Caltech and MIT with funding from NSF under cooperative agreement PHY 9210038. The LIGO Laboratory operates under cooperative agreement PHY-0107417. This paper has been assigned LIGO document number LIGO-P030022-00-D.

REFERENCES

Berger, E., et al., 2003, ApJ, 588, 99

Blain, A.W., & Natarajan, P., 2000, MNRAS, 312, L39

Bloom, J.S., et al, 1999, Nature, 401, 453

Bromm, J.S & Loeb, A., 2002, ApJ, 575, 111

Choudhury, T.R., & Srianand, R., 2002, MNRAS, 336, L27

Coward, D.M., Burman, R.R., Blair, D.G., 2002, MNRAS, 329, 411

de Bernardis, P., et al, 2000, Nature 404, 995

Frail, D.A., et al., 2001, ApJ, 562, L55

Freedman W., et al., 2001, Astrophys. J. 553, 47

Fruchter, A.S., et al., 1999, ApJ, 519, L13

Galama, T.J., et al, 1998, Nature, 395, 670

Hanany, S., et al, 2000, ApJ, L545, 5

Heger, A., Fryer, C.L., Woosley, S.E., Langer, N., & Hartmann, D.H., 2002, submitted (astro-ph/0212469)

Kulkarni, S.R., et al, 2000, Proc.SPIE, 4005, 9

Levinson, A., Ofek, E., Waxman, E., Gal-Yam, A., 2002, ApJ, 576, 923

Perlmutter, S., et al, 1999, ApJ, 517, 565

Porciani, C., & Madau, P., 2001, ApJ, 548, 522

Paczynsky B., 1998, ApJ, 494, L45

Reichart, D.E., 2001, ApJ, 554, 643

Rossi, E., Lazzati, D., & Rees, M.J., 2002a, MNRAS, 332, 945

Schmidt, B., et al, 1998, ApJ, 507, 46

Sethi, & Bhargavi, 2001, A&A, 376, 10

Stanek, K.Z., et al., 2003, astro-ph/0304173

Woosley, S., 1993, ApJ, 405, 273

Zhang, B., & Meszaros, P., 2002, ApJ, 571, 876

Table 1. A sample of 33 GRBs with individually determined redshifts ^a

GRB	Redshift z	Photon flux ^b	Luminosity ^c	θ_j ^d	Instrument
970228	0.695	10	2.13×10^{58}		SAX/WFC
970508	0.835	0.97	3.24×10^{57}	0.293	SAX/WFC
970828	0.9578	1.5	7.04×10^{57}	0.072	RXTE/ASM
971214	3.42	1.96	2.08×10^{59}	> 0.056	SAX/WFC
980425	0.0085	0.96	1.54×10^{53}		SAX/WFC
980613	1.096	0.5	3.28×10^{57}	> 0.127	SAX/WFC
980703	0.966	2.40	1.15×10^{58}	0.135	RXTE/ASM
990123	1.6	16.41	2.74×10^{59}	0.050	SAX/WFC
990506	1.3	18.56	1.85×10^{59}		BAT/PCA
990510	1.619	8.16	1.40×10^{59}	0.053	SAX/WFC
990705	0.86			0.054	SAX/WFC
990712	0.434	11.64	7.97×10^{57}	> 0.411	SAX/WFC
991208	0.706	11.2*	2.48×10^{58}	< 0.079	Uly/KO/NE
991216	1.02	67.5	3.70×10^{59}	0.051	BAT/PCA
000131	4.5	1.5*	3.05×10^{59}	< 0.047	Uly/KO/NE
000210	0.846	29.9	1.03×10^{59}		SAX/WFC
000301C	0.42	1.32*	8.37×10^{56}	0.105	ASM/Uly
000214	2.03				SAX/WFC
000418	1.118	3.3*	2.27×10^{58}	0.198	Uly/KO/NE
000911	1.058	2.86	1.72×10^{58}		Uly/KO/NE
000926	2.066	10*	3.13×10^{59}	0.051	Uly/KO/NE
010222	1.477				SAX/WFC
010921	0.45				HE/Uly/SAX
011121	0.36	15.04*	6.63×10^{57}		SAX/WFC
011211	2.14				SAX/WFC
020405	0.69	7.52*	1.58×10^{58}		Uly/MO/SAX
020813	1.25	9.02*	8.19×10^{58}		HETE
021004	2.3				HETE
021211	1.01				HETE
030226	1.98	0.48*	1.35×10^{58}		HETE
030323	3.37	0.0048*	4.91×10^{56}		HETE
030328	1.52	2.93*	4.31×10^{58}		HETE
030329	0.168	0.0009*	7.03×10^{52}		HETE

^aCompiled from S. Barthelmy’s IPN redshifts and fluxes (<http://gcn.gsfc.nasa.gov/gcn/>) and J.C. Greiner’s catalogue on GRBs localized with WFC (BeppoSax), BATSE/RXTE or ASM/RXTE, IPN, HETE-II or INTEGRAL (<http://www.mpe.mpg.de/jcg/grbgeb.html>)

^bin $\text{cm}^{-2}\text{s}^{-1}$

^cPhoton luminosities in s^{-1} derived from the measured redshifts and observed gamma-ray fluxes for the cosmological model described in §2

^dOpening angles θ_j in the GRB-emissions refer to the sample listed in Table I of Frail et al.(2001).

*Extrapolated to the BATSE energy range 50 - 300 keV using the formula given in Appendix B of Sethi et Bhargavi (2001)

Figure Captions

Figure 1. Shown are three redshift distributions: the observed sample derived from Table 1 (white), the true sample assuming the GRB event rate is locked to the star-formation rate (hachured), and the sample of detectable GRBs predicted by our model according to a log-normal peak-luminosity distribution function (grey). The continuous line represents the cosmic star formation rate according to a Λ -dominated cold dark matter universe.

Figure 2. Shown is a simulation of the redshift distribution of the observed GRBs as a function of flux-limit, corresponding to various instruments including the upcoming SWIFT mission. The results are derived assuming the GRB event rate to be locked to the star-formation rate, using the best fit log-normal peak-luminosity distribution function used in Fig. 2. HETE-II thresholds are 0.21 (SXC), 0.07 (WXM) and 0.3 (FREGATE) in units of $\text{cm}^{-2}\text{s}^{-1}$.

Figure 3. Shown is a comparison between the flux distributions derived from our model (in grey) and from a sample of 67 GRBs observed with IPN (in white). The fit serves as a test for our model assumptions, namely a log-normal GRB-luminosity function and a GRB event rate locked to the star-formation rate.

Figure 4. Shown is a plot of the opening angle θ_j of GRB-emissions versus redshift z in the sample of Frail et al. (2001), as derived from achromatic breaks in the GRB light curves. These results indicate an anticorrelation between θ_j and z . For standard GRB-energies, this introduces a peak-luminosity function of GRBs which is correlated with the beaming factor $1/f_b$. This allows the beaming factor to be determined also in terms of the ratio of the unseen-but-true GRB event rate to the observed GRB event rate, using the current flux-limited sample of 33 GRBs with individually measured redshifts.

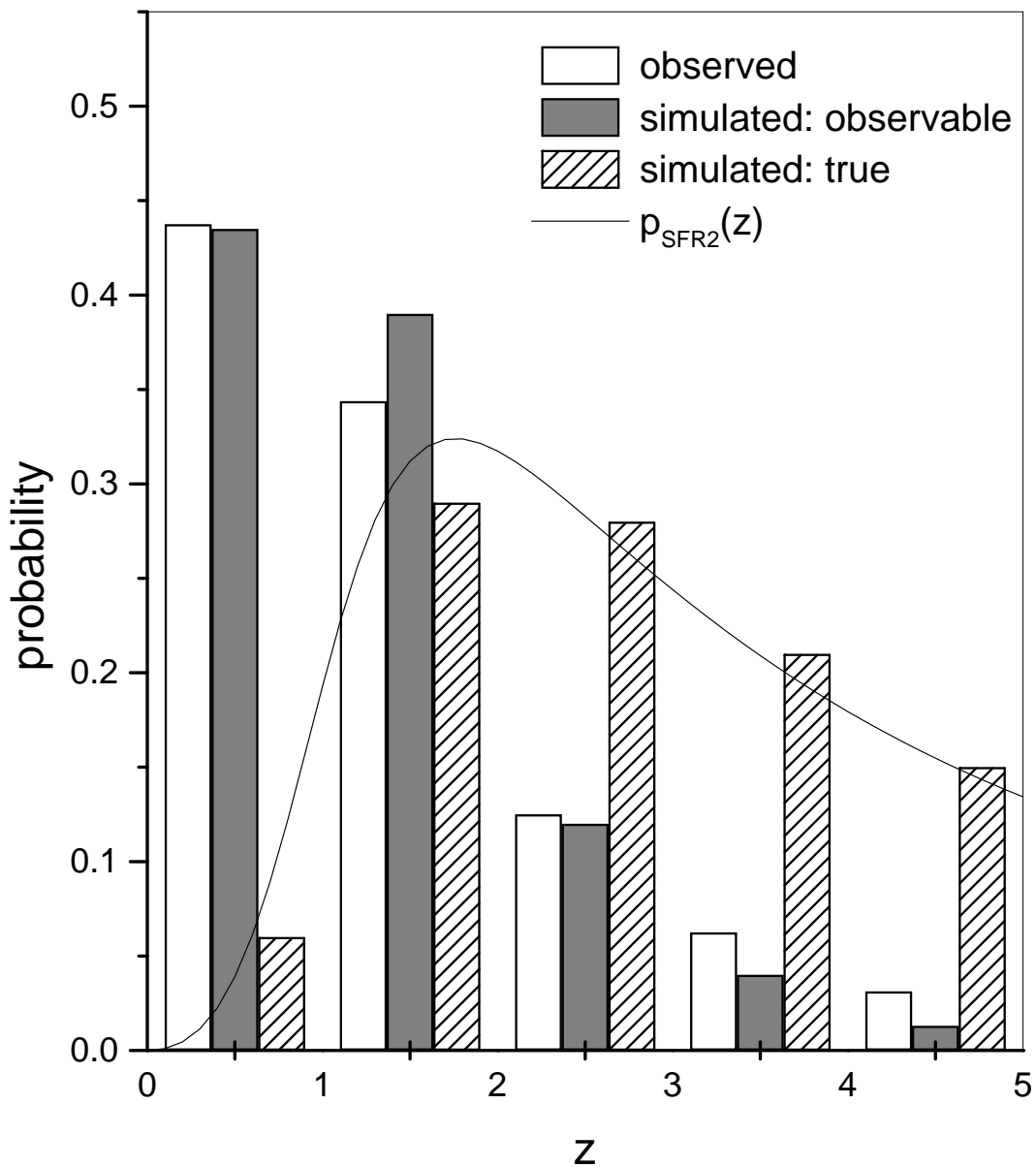


Fig. 1.—

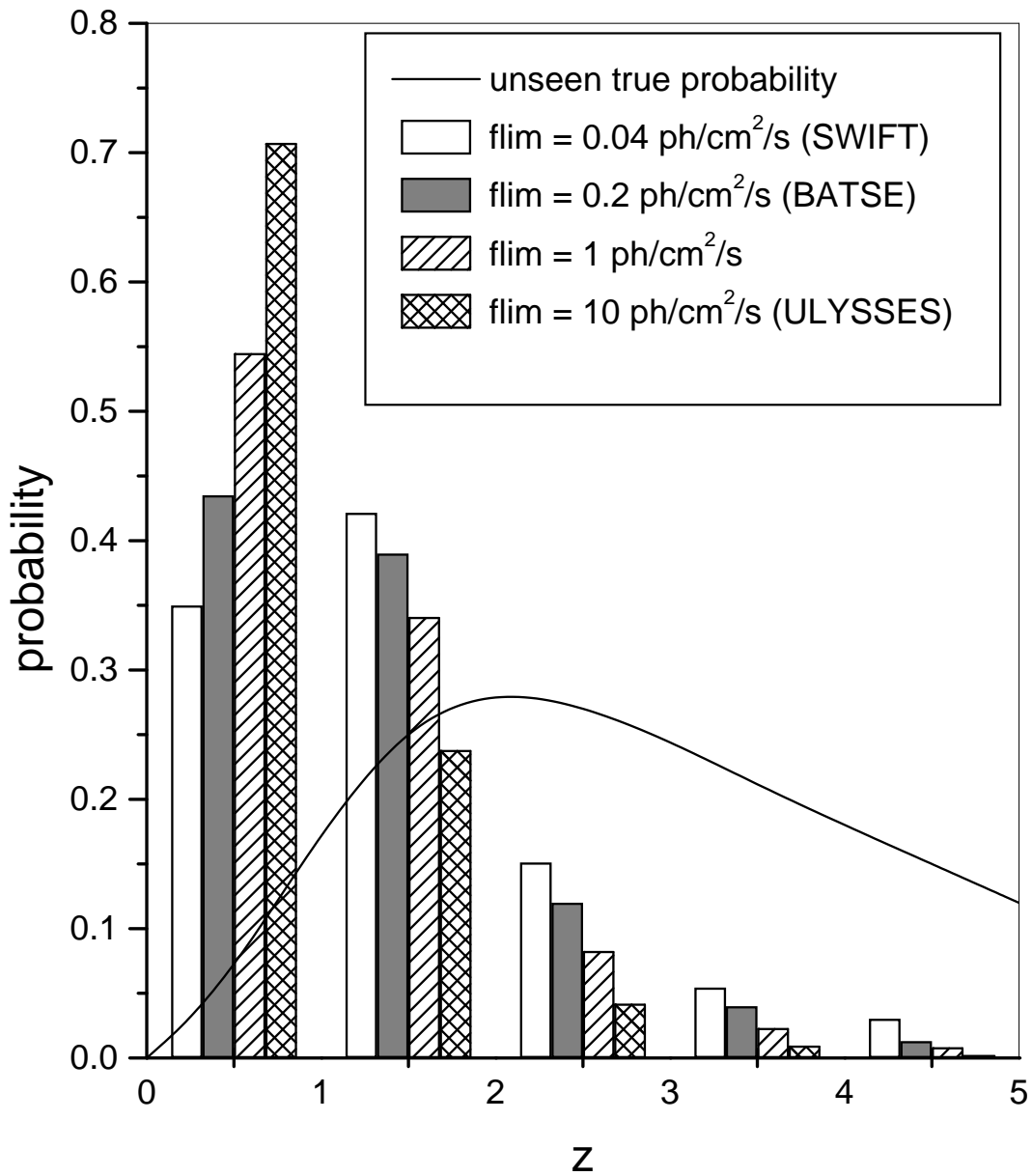


Fig. 2.—

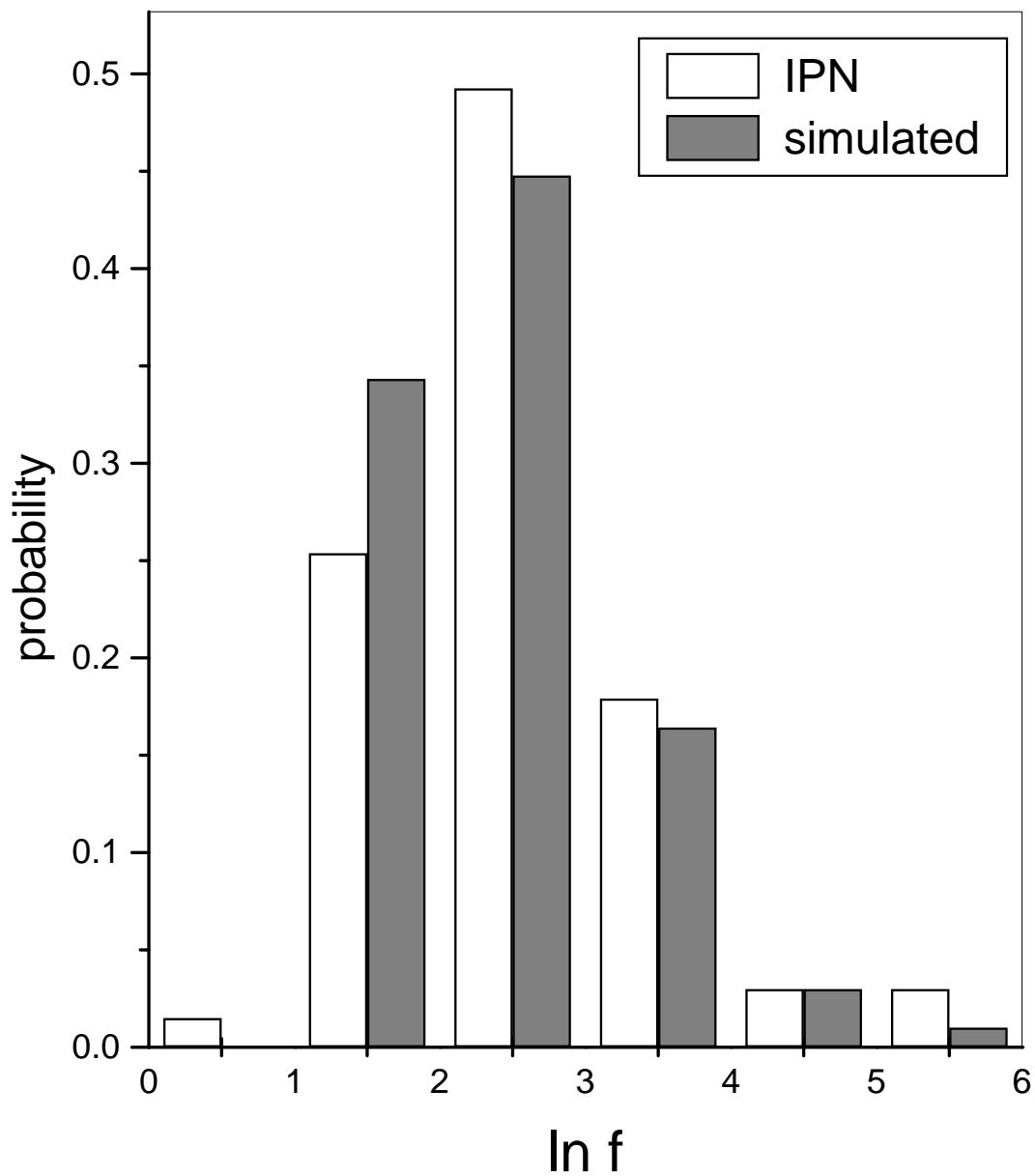


Fig. 3.—

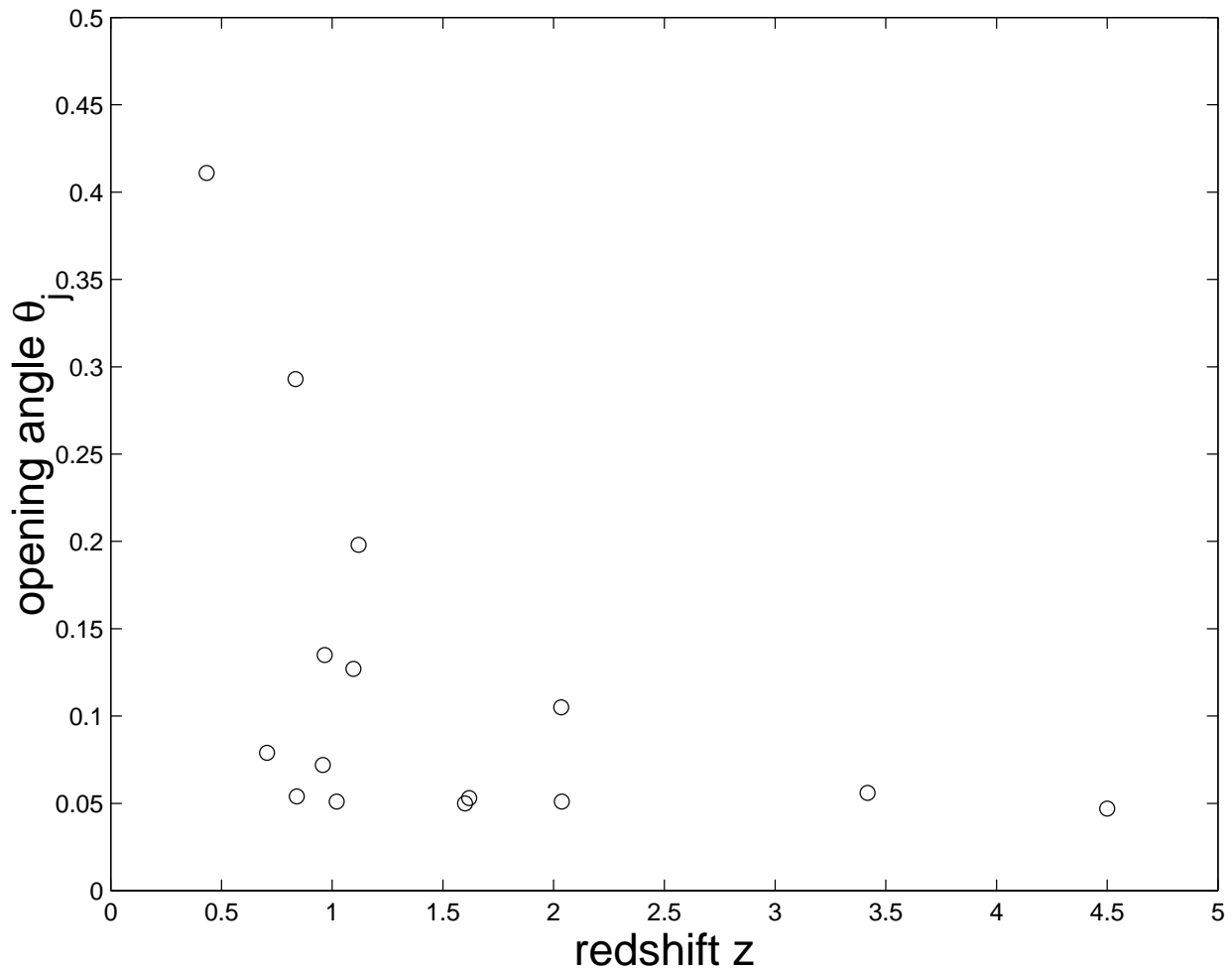


Fig. 4.—